Experimental Methods for UAV Aerodynamic and Propulsion Performance Assessment

Stefan ANTON*,[1], Petrisor PARVU[1]

*,[1]"POLITEHNICA" University of Bucharest, Faculty of Aerospace Engineering
Polizu Street 1-7, sector 1, Bucharest 011061, Romania
stefan.anton88@yahoo.com*, parvu@aero.pub.ro

DOI: 10.13111/2066-8201.2015.7.2.2

3rd International Workshop on Numerical Modelling in Aerospace Sciences, NMAS 2015,
06-07 May 2015, Bucharest, Romania, (held at INCAS, B-dul Iuliu Maniu 220, sector 6)
Section 5 – New concepts in UAV systems

Abstract*: This paper presents an experimental method for assessing the performances and the propulsion power of a UAV in several points based on telemetry. The points in which we make the estimations are chosen based on several criteria and the fallowing parameters are measured: airspeed, time-to-climb, altitude and the horizontal distance. With the estimated propulsion power and knowing the shaft motor power, the propeller efficiency is determined at several speed values. The shaft motor power was measured in the lab using the propeller as a break. Many flights, using the same UAV configuration, were performed before extracting flight data, in order to reduce the instrumental or statistic errors. This paper highlights both the methodology of processing the data and the validation of theoretical results*.

Key Words: *aerodynamic performance, propulsion performance, airspeed indicator, gliding flight, horizontal flight, motor measurement, aeropropulsiv model*

1. INTRODUCTION

Flight tests are one of the most challenging engineering problems. They involve team work and the recognition of the fact that sometimes the collective judgment outweighs the advantage of quick decisions taken by a single individual. Flight tests are needed to determine the actual characteristics of the airplane and compared to computed or predicted characteristics, they help to provide further development information and to obtain research information. Because of the need to verify all theoretical and computed results the FLIGHT tests are likely to be an integral part of the development of most aerospace vehicles.

Flight tests must be carefully planned in order to keep safety, cost and schedule considerations in balance [2].

The atmospheric conditions determine the performances and handling qualities of an aircraft and so they have a major impact over the flight tests. Because two flight tests never produce the same result, the data must be carefully reduced to the standard conditions. The instruments that are affected by the atmospheric conditions are the altimeter and the speed indicator [2].

Because there is a variety of altitude types used in literature they will be discussed in order to eliminate ambiguity [2]:

Geometric altitude (true altitude) h_g: is the vertical distance from the mean sea level to the point in question;

Pressure altitude, h_p: is the geometric altitude in a standard atmosphere at which a given pressure is found. A properly calibrated altimeter indicates the pressure altitude;

Density altitude h_ρ is the geometric altitude in a standard atmosphere at which a given density occurs. Unlike pressure, the density is measured indirectly (measure of pressure and temperature). Density altitude is used to predict available thrust or power from the propulsion system;

Absolute altitude, h_s: is the distance measured from the center of the earth to the point in question. This altitude is a prime concern in orbital mechanics because the local gravitational acceleration, g, is a function of altitude;

Geo-potential altitude, h: is a fictitious altitude obtained from geometric altitude by assuming g is a constant from the mean sea level up to any altitude.

$h = \left(\frac{R_E}{R_E + h_g} \right) h_g$, where R_E is the radius of the earth.

2. AIRSPEED THEORY

Both altitude and airspeed measuring systems are typically pressure sensing systems. An airspeed indicator (ASI) measures the differential pressure while an altimeter measures the absolute pressure; both use the same static pressure source.

Considering Euler's equation [2] for steady, streamline flow:

$$\frac{dp}{\rho} + VdV = 0 \tag{1}$$

Integrating gives either the incompressible or the compressible Bernoulli equation:

$$p + \frac{\rho V^2}{2} = ct \ \ (\textbf{Incompressible}) \text{ or } \int \frac{dp}{\rho} + \frac{\rho V^2}{2} = ct \ \ (\textbf{compressible}) \tag{2}$$

For an isentropic process, $\left(\frac{p}{\rho} \right)^y = \left(\frac{p_T}{\rho_T} \right)^y = ct$. a convenient form of the compressible Bernoulli equation results after solving for ρ and integrating:

$$\frac{\gamma \cdot p}{\rho(\gamma - 1)} + \frac{V^2}{2} = ct \tag{3}$$

If eq. (3) is applied to the flow into the total head orifice of the ASI where $V_\infty = 0$ and to the streamline flow past the static orifices in the pitot-static system

$$\frac{\gamma \cdot p}{\rho(\gamma - 1)} + \frac{V^2}{2} = \frac{\gamma \cdot p_T}{\rho_T(\gamma - 1)} \tag{4}$$

The differential pressure sensed by a conventional pitot-static system, q_c, is not simply the dynamic pressure, though it has a similar form.

$$q_c = p_T - p = p\left(\frac{p_T}{p} - 1 \right) \tag{5}$$

Isentropically,

$$\frac{p_T}{p} = \left(1 + \frac{\gamma - 1}{2} M^2\right)^{\frac{\gamma}{\gamma - 1}} \tag{6}$$

Solving for V and multiplying both sides by $\sqrt{\sigma} = \sqrt{\frac{\rho}{\rho_0}}$:

$$V\sqrt{\sigma} = \sqrt{\frac{2 \cdot \gamma \cdot p}{(\gamma - 1)\rho_0}\left(\frac{q_c}{p} + 1\right)^{\frac{\gamma}{\gamma - 1}} - 1} \tag{7}$$

A Careful examination of eq. (7) reveals that calibrating a differential pressure gage [2] (which the ASI is) in velocity units is not as easy as it may seem. Pressure and/or density are different at each pressure altitude and, even with V as the measure of velocity it means that a new scale would be needed for each pressure altitude. Such scaling is obviously impractical and so a scale based on standard day sea level conditions is defined by [2]:

$$V_{cal} = V\sqrt{\sigma}\,|_{\rho=\rho_0} \text{ -calibrated airspeed} \tag{8}$$

where $\sqrt{\sigma}$ is evaluated at the standard day sea level pressure.

Equivalent airspeed is the name given to $V\sqrt{\sigma}$ and is a direct measure of the kinetic energy of the volume V of moving fluid:

$$V\sqrt{\sigma} = V_e \tag{9}$$

Equivalent airspeed appears in all force and moment equations and therefore commonly correlates directly to structural loads on the airframe.

One final type of airspeed, Indicated airspeed must be defined for the flight test data reduction. It is simply the dial reading from the specific differential pressure gauge used. Each such gauge used in experimental work should be periodically calibrated as compared to a known differential pressure source (8). Altimeter should also be periodically calibrated in a similar manner. [2]

3. PITOT MEASUREMENTS ERRORS

- instrumental error;
- pressure lag error;
- position error.

Instrumental error

The Instrumental error is simply the deviation of the instrument indications from a known differential pressure standard. It results from imperfections in the gauge itself and is typically measured in a calibration laboratory with the instrument disconnected from other parts of the pitot-static system. Several factors contribute to the instrument error such as: the scale error, manufacturing deviations, magnetic fields, temperature fluctuations, coulomb and viscous friction, and the inertia of the moving parts. The instrument corrections are usually given as the differences between the instruments corrected values and the gauge readings:

$\Delta V_{ic} = V_{ic} - V_i$;

V_{ic} - calibrated airspeed using a laboratory for the reading I;

V_i -gauge reading at a given condition.

These corrections can be either positive or negative depending on the particular instrument. A typical altimeter correction[2] curve is given in Fig 1.

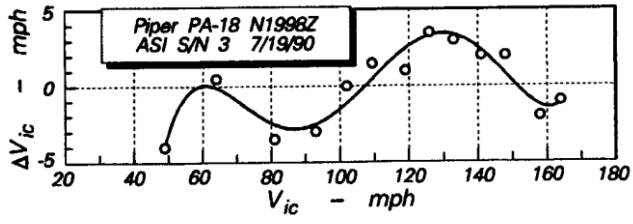

Fig. 1 Typical altimeter correction

Pressure lag error

Any pressure sensing system, like the conventional aircraft pitot-static system, is subject to errors due to time delaying transmitting the pressure from the point of measurement to the sensor. In an airplane, this error is typically only when the rates of the pressure changing of pressure are high. The lag error is proportional to the pressure drop through the system lines from the pressure orifice to the pressure indicator.

Position error

Position error calibration methods:

Free stream static pressure methods in which the pressure difference (ΔP) is obtained from the measurement of the static pressure and P_{∞}.

True airspeed method in which ΔP is derived from the values of V_{∞} calculated from groundspeed measurements.

A temperature method in which ΔP is determined from the measured temperature and a pressure-temperature survey.

Mach number methods, in which ΔP is obtained from the Mach number.

Of these four types of calibrations methods the first two are the most commonly used. They are especially well-suited for low speed and low altitude, although the first category of methods includes several techniques useful at high altitudes and airspeed.

4. EXPERIMENTAL VERSUS ANALYTICAL PERFORMANCE METHODS

Performance measurements have little meaning unless the data are reduced to some common basis of comparison [2]. This common basis is the standard atmosphere. Hence, the performance reduction refers to the data reduction schemes by which the test data taken under nonstandard day conditions are converted to standard day results.

There are two broad categories of performance data reduction. Experimental methods are so named because they do not require knowing in advance the components of the dynamical system. For an airplane, for example, no knowledge of the power plant characteristics would be required under this method. Analytical methods do require a priori sources to complete the analysis and are somewhat more widely used. Analytical methods are further broken down into differential methods and performance analyses. Differential methods are based on the notion that for small corrections, linearization is appropriate. These

methods depend on a generalized characterization of airframe drag and engine behavior. The Performances analyses rely on advance information of the engine behavior and are generally used while experimental methods are inconvenient or simply impractical.

One of most perplexing problems in performance reduction is the number and type of variables to be considered, some of which are controllable while others are not. Engine parameters are, for example, usually quite controllable over the range of interest but outside air temperature is not. Tests are ordinarily planned to cover a suitable range of the controllable variables, while those variables that cannot be controlled are "standardized".

5. GLIDING FLIGHT FOR A FLYING WING

Every airplane on every flight; takes off, climbs, turns, descends and lands. Thus, immediately after the pitot-static system is calibrated the test team can begin collecting performance data for these phases of flight. The descent performance of a vehicle is of utmost importance to the operator and is directly related to lift and drag. Generally, measurements are made to determine either a speed or Mach number profile, minimum fuel to altitude or minimum time to a total energy level. The actual altitude and velocity measurements can be manipulated to describe the maneuver capability of the airplane or to evaluate the tactical capability of the vehicle relative to an adversary.

Gliding flight equations [3]

$$\begin{aligned} \frac{\rho}{2} \cdot S \cdot V^2 \cdot C_Z &= G \cdot \cos(\gamma) \\ \frac{\rho}{2} \cdot S \cdot V^2 \cdot C_X &= G \cdot \sin(\gamma) \end{aligned} \tag{10}$$

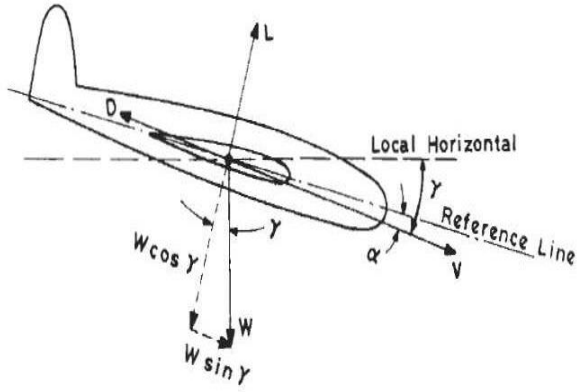

Fig. 2 Forces and angles for gliding flight

we add the parabolic drag polar [5] at these equations:

$$C_X(C_Z) = C_{X_{\min}} + \frac{1}{\pi \cdot Ar \cdot e} \cdot (C_Z - C_{Z_{\min}})^2 \tag{11}$$

From (10) and (11) we obtain an equation between $C_{X_{\min}}$, $C_{Z_{\min}}$ and the e Oswald's coefficient, which is valid for any speed ranging between V_{min} si V_{max}.

$$\frac{G \cdot \sin(\gamma)}{\frac{\rho}{2} \cdot S \cdot V^2} = C_{X_{\min}} + \frac{1}{\pi \cdot Ar \cdot e} \cdot \left(\frac{G \cdot \cos(\gamma)}{\frac{\rho}{2} \cdot S \cdot V^2} - C_{Z_{\min}} \right)^2 \tag{12}$$

The airspeed values and gliding path corresponding to these speeds are extracted from the following telemetry data:

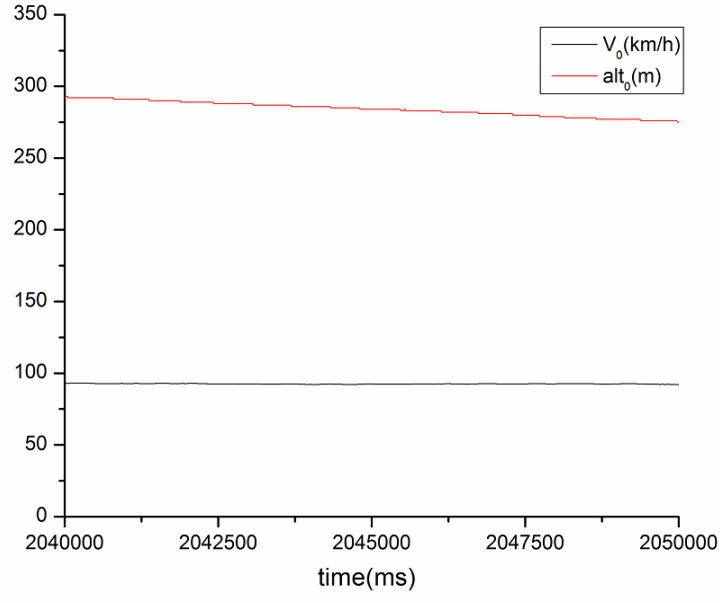

Fig. 3 Airspeed and altitude drop for the first gliding segment

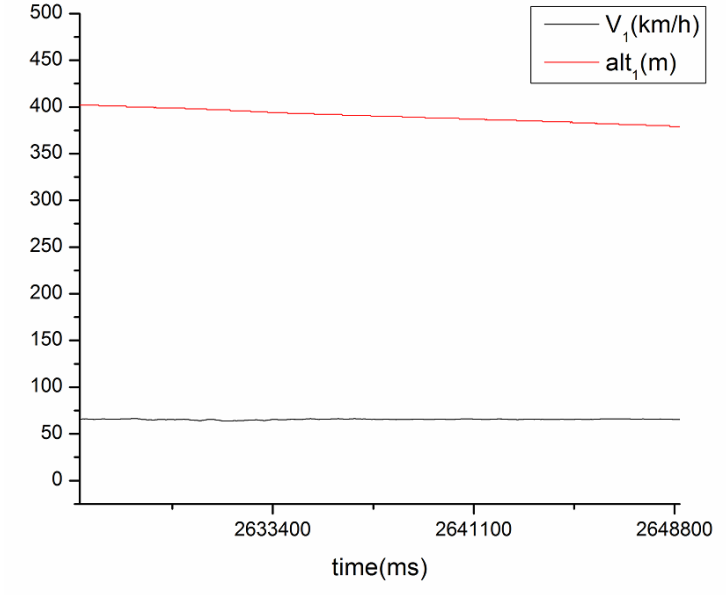

Fig. 4 Airspeed and altitude drop for the second gliding segment

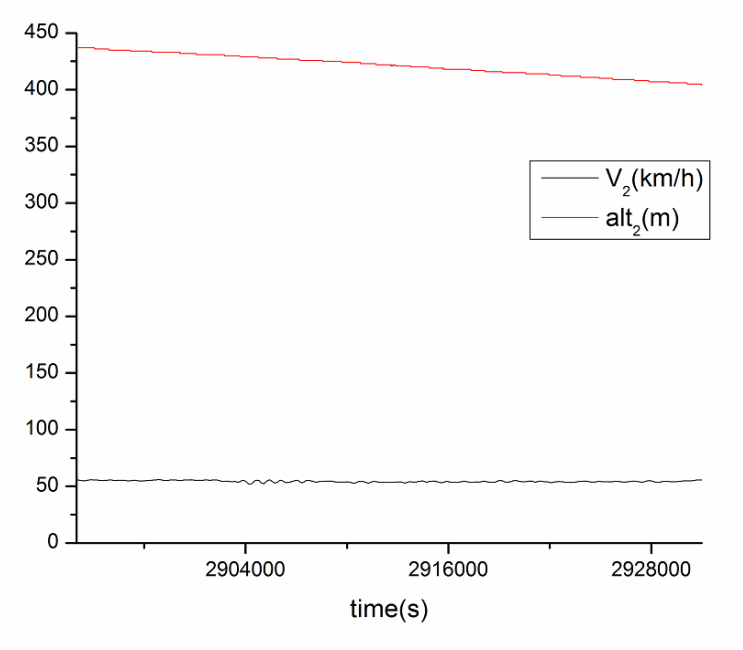

Fig. 5 Airspeed and altitude drop for the third gliding segment

There were extracted 3 flight segments that respect the following criteria:

- Pitch and roll close to 0;
- Yaw and *V* constant;
- Trajectory in straight line;

The flight segment must be long enough so that the movement history won't influence the speed.

$$\gamma = \begin{pmatrix} 3.883 \\ 3.129 \\ 3.305 \end{pmatrix} \cdot \deg\,,\; V = \begin{pmatrix} 25.694 \\ 18.306 \\ 15.278 \end{pmatrix} \tag{13}$$

Using the equation solver from Mathcad:

Given

$$\frac{G \cdot \sin(\gamma)}{\frac{\rho}{2} \cdot S \cdot V^2} = C_{X_{\min}} + \frac{1}{\pi \cdot Ar \cdot e} \cdot \left(\frac{G \cdot \cos(\gamma)}{\frac{\rho}{2} \cdot S \cdot V^2} - C_{Z_{\min}} \right)^2$$

$$\begin{pmatrix} C_{Z_{\min}} \\ C_{X_{\min}} \\ e \end{pmatrix} = Find(C_{Z_{\min}}, C_{X_{\min}}, e) \tag{14}$$

where *V* and γ are the above vectors (13) and $G = 42N,\ S = 0.761m^2,\ \rho = 1.225\frac{kg}{m^3}$ and $Ar = 9.438$.

The following solution resulted for $C_{X_{\min}}, C_{Z_{\min}}$ and Oswald coefficient *e*.

$$C_{Z_{\min}} = -0.246$$
$$C_{X_{\min}} = 2.728 \cdot 10^{-3} \quad (15)$$
$$e = 0.794$$

Therefore the equation (11) which is obtained with the above mentioned coefficients is compared with the results from XFLR in the graphic below:

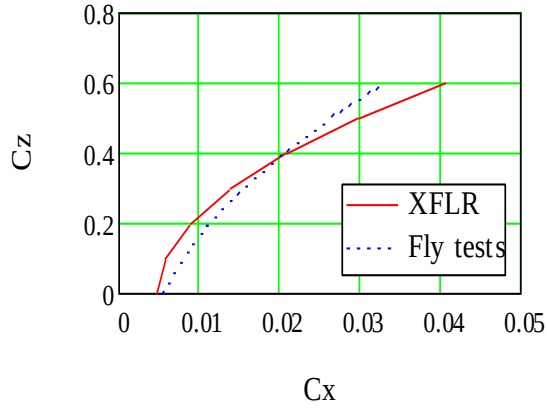

Fig. 6 Drag polar

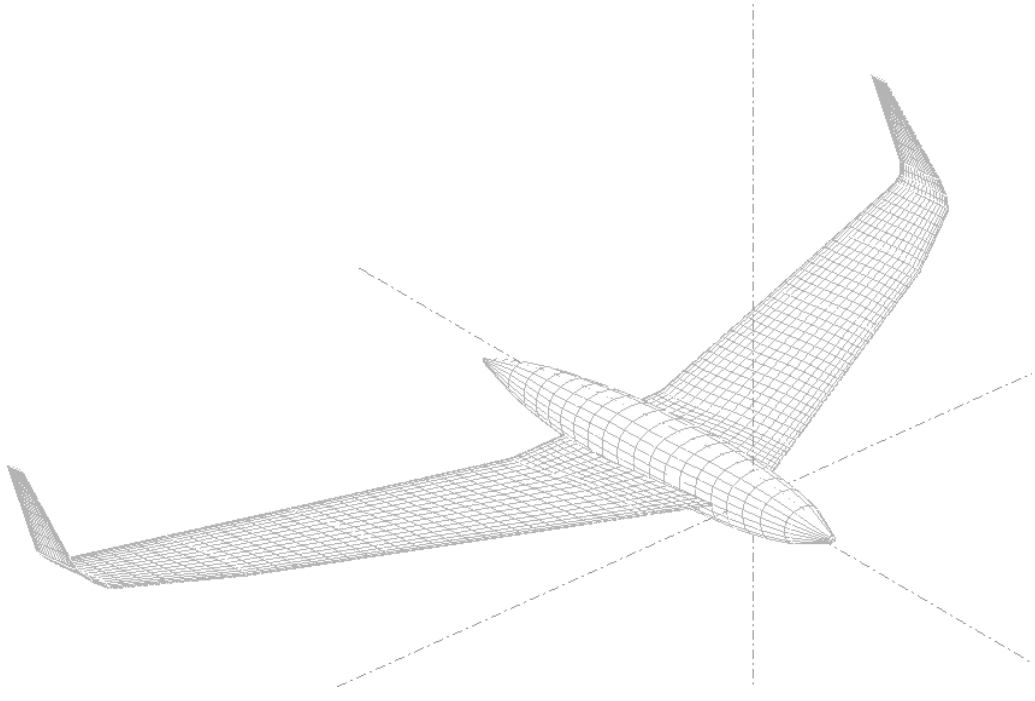

Fig. 7 XFLR Model

The results differ significantly for various reasons:

- The polar in XFLR is estimated by the VLM method, which involves several approximations and also the fuselage geometry input is approximated.

- Geometrical differences due to execution reasons on real plane. In this case we can enumerate the following: the trailing edge of the wing is thicker than the theoretical one, the motor controller radiator is positioned in the airflow, etc.
- Measurement errors of speed and altitude

The method relies on matching the parable in 3 points which means that the values for *Cx* and *Cz* between the calculation points are approximate.

The more flight data we have to fully satisfy the selection criteria the more accurate our results will be.

6. HORIZONTAL FLIGHT

In the case of horizontal flight, besides the (11) relation, I also have introduced the traction variation depending on speed (17).

Therefore starting from the horizontal flight equations [3] (16), using (17) and adding the variation of drag coefficient depending on lift coeficient (11):

$$\begin{aligned} \frac{\rho}{2} \cdot S \cdot V^2 \cdot C_Z &= G \\ \frac{\rho}{2} \cdot S \cdot V^2 \cdot C_X &= T \end{aligned} \tag{16}$$

$$T(V) = k_0 + k_1 \cdot V + k_2 \cdot V^2 \tag{17}$$

we obtain the following equation:

$$T(V) = \frac{\rho}{2} \cdot S \cdot V^2 \cdot \left[C_{X_{\min}} + \frac{1}{\pi \cdot Ar \cdot e} \cdot \left[\frac{G}{\left(\frac{\rho}{2} \cdot S \cdot V^2 \right)} - C_{Z_{\min}} \right]^2 \right] \tag{18}$$

The above equation has as unknowns: k_0, k_1, k_2, $C_{X_{\min}}$, $C_{Z_{\min}}$ and e that are valid for any V speed in the range $V_{\min} - V_{\max}$. Therefore we have to solve a system of 6 equations with 6 unknowns.

The numerical solution of this system presents singularities problems; for a small variation of the initial values we encounter a significant variation of solutions which didn't happen during the gliding flight.

One method of solving the system is to match the values for an initial speed and afterwards to change them in order to match to the other speeds.

The solving idea derives from the article *"Using flight manual data to derive aero-propulsive models for predicting aircraft trajectories"* written by Chester Gong and William N. Chan[1].

This article presents a method in which the flight manual data are used in order to obtain predictions about trajectories by building an aeropropulsive model. The determination method of aerodynamic coefficient ($C_{X_{\min}}, C_{Z_{\min}}$ and e) and of propulsive coefficient, k, is presented in the picture[1] below:

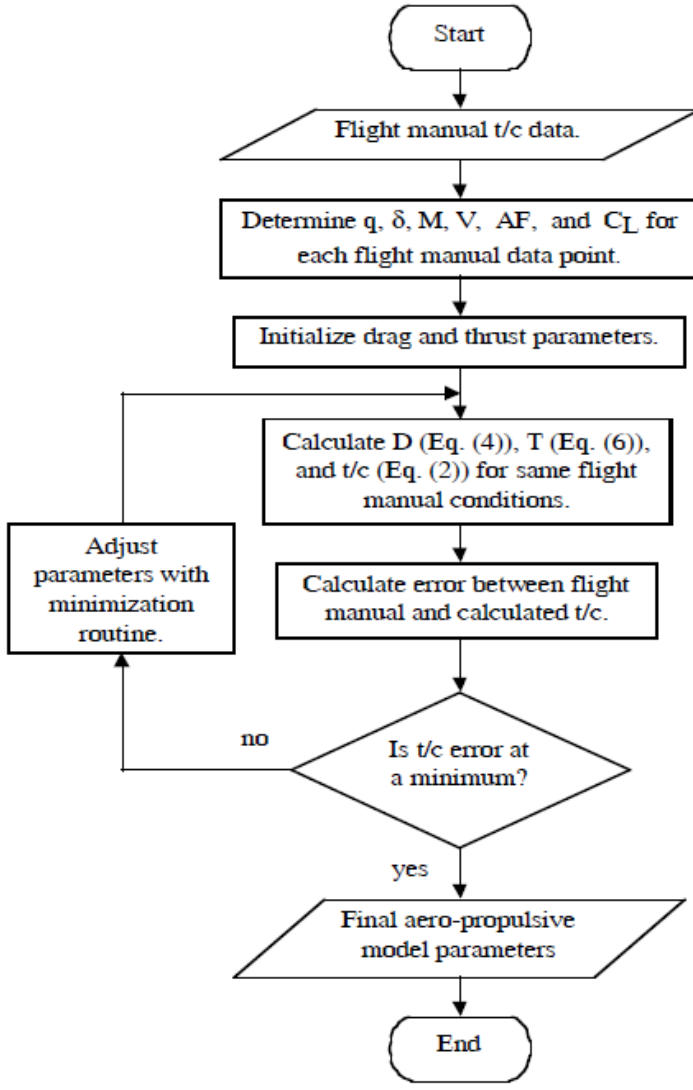

Fig. 8 Gong method

in which data from the flight manual are provided as follows [1,4]:

Table 1 – Sample climb data for a Learjet 60

Altitude (1000 ft)	Time (min)	Distance (nm)	Fuel (lb)
47	22.3	141.0	639.8
45	14.9	91.8	513.7
43	12.4	75.2	465.4
.	.	.	.
.	.	.	.
.	.	.	.
5	0.8	3.6	49.9
3	0.5	2.1	30.2
1	0.2	0.7	10.2

and equations 2, 4 and 6 are[1]:

$$T = \delta \cdot \left(\frac{T}{\delta}\right) = \delta \cdot K \cdot \left(\frac{T}{\delta}\right)$$

$$D = \left[C_{X_{\min}} + \frac{(C_Z - C_{X_{\min}})^2}{\pi \cdot Ar \cdot e \cdot \sqrt{1 - M^2}} \right] \cdot q \cdot S$$

$$tc = \int \frac{1 + AF}{\left(\frac{T - D}{W}\right) \cdot V} dh$$

The method was applied on Learjet 60 and the results were validated by RADAR tracking. The results for the 4 unknowns are illustrated below [1, 4]:

Table 2 - Model parameters for the Learjet 60

Parameters	Values
C_{Dmin}	0.015
C_{Lmin}	0.12
e	0.71
K	0.22

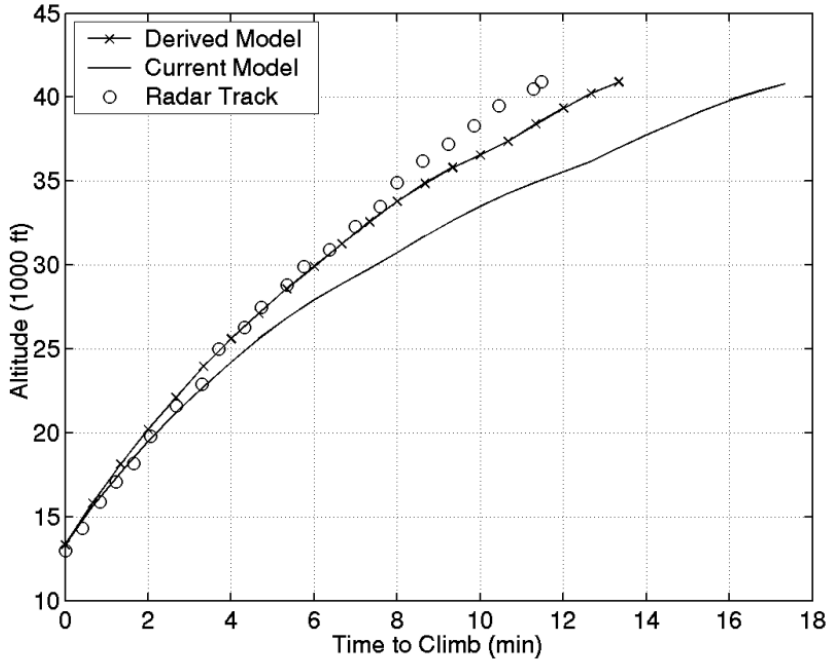

Fig. 9 Radar track vs aeropropulsiv model [1]

Since the numerical solving of the system is not easy, we can use $C_{X_{\min}}$, $C_{Z_{\min}}$ and e determined at the gliding flight, thus it will only remain to solve the unknowns k_0, k_1, k_2. Therefore we have to solve a system of 3 equations with 3 unknowns:

$$T_0 = \frac{\rho}{2} \cdot S \cdot (V_0)^2 \cdot \left[C_{X_{min}} + \frac{1}{\pi \cdot Ar \cdot e} \cdot \left[\frac{G}{\left[\frac{\rho}{2} \cdot S \cdot (V_0)^2 \right]} - C_{Z_{min}} \right]^2 \right]$$

$$T1 = \frac{\rho}{2} \cdot S \cdot (V_1)^2 \cdot \left[C_{X_{min}} + \frac{1}{\pi \cdot Ar \cdot e} \cdot \left[\frac{G}{\left[\frac{\rho}{2} \cdot S \cdot (V_1)^2 \right]} - C_{Z_{min}} \right]^2 \right] \quad (19)$$

$$T_2 = \frac{\rho}{2} \cdot S \cdot (V_2)^2 \cdot \left[C_{X_{min}} + \frac{1}{\pi \cdot Ar \cdot e} \cdot \left[\frac{G}{\left[\frac{\rho}{2} \cdot S \cdot (V_2)^2 \right]} - C_{Z_{min}} \right]^2 \right]$$

with the following solutions for the traction T:

$$T = \begin{pmatrix} 2.739 \\ 2.174 \\ 2.132 \end{pmatrix} \quad (20)$$

From equations (12) and T (values from above) results A system with 3 equations and 3 unknowns: k_0 , k_1, k_2 results from equations (12) and T (values from above):

$$\begin{aligned} T_0 &= k_1 \cdot V_0 + k_2 \cdot (V_0)^2 + k_0 \\ T_1 &= k_1 \cdot V_1 + k_2 \cdot (V_1)^2 + k_0 \\ T_2 &= k_1 \cdot V_2 + k_2 \cdot (V_2)^2 + k_0 \end{aligned} \quad (21)$$

$$\begin{aligned} k_0 &= 3.596 \\ k_1 &= -0.188 \\ k_2 &= 5.999 \cdot 10^{-3} \end{aligned} \quad (22)$$

With determined k_0 , k_1, k_2 values we can build the *T(V)* graph:

$$T(V) = k_1 \cdot V + k_2 \cdot (V)^2 + k_0$$

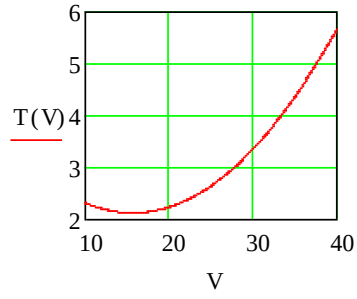

Fig. 10 T (V) graph

7. MOTOR MEASUREMENTS

Once we know the 6 parameters $C_{X_{\min}}$, $C_{Z_{\min}}$, e, k_0, k_1 and k_2 we can estimate the propeller efficiency.

First of all we need to estimate the motor efficiency depending on the electric power supplied by the accumulators and the RPM.

For the motor used in gliding flight AXI 2826/10, measurements were taken and the table below resulted.

Different propellers were used as a brake, the RPM was measured and after its stabilization we could read the following parameters: *m* (the weight indicated by the weight scale), *I* (current intensity) and *Pe* (electric power).

Knowing mechanical torque and consumed electric power we were able to calculate the motor efficiency.

MOTOR AXI 2826-10 , 4 LIPO , JETI 77-PRO

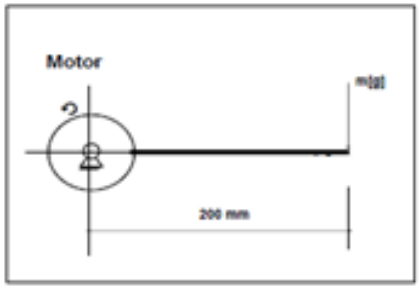

Pm[w] = 0.205 x n/1000 [rot/min] x m[g]
η[%] = Pm /Pe x 100

Propeller	Measured (±2%) n [rot/min]	m [g]	I [A]	P_e [w]	Calculated P_m [w]	η [%]
8/6"	6000	18	3.2	48	22.1	46.1
	7040	24	4.9	72	34.6	48.1
	8100	32	6.9	102	53.1	52.1
	9000	40	8.8	130	73.8	56.8
	10000	50	11	163	102.5	62.9
	11000	62	13.8	204	139.8	68.5
	12000	75.5	17	252	185.7	73.7
	12530	82.5	18.9	280	211.9	75.7
9.5/6"	6050	36	5.2	77	44.6	58.0
	7010	49	7.4	110	70.4	64.0
	8040	63.5	10.2	151	104.7	69.3
	9000	78	13.3	197	143.9	73.1
	10000	94	17	252	192.7	76.5
	11000	111	21.4	317	250.3	79.0
	11750	125	25.3	374	301.1	80.5
11/7"	6000	69	10.1	149	84.9	57.0
	7040	97	15.1	224	140.0	62.5
	8050	128	20.9	309	211.2	68.4
	9000	160	27.2	402	295.2	73.4
	10000	200	35.1	520	410.0	78.8

Fig. 11 AXI 2826-10 measurements

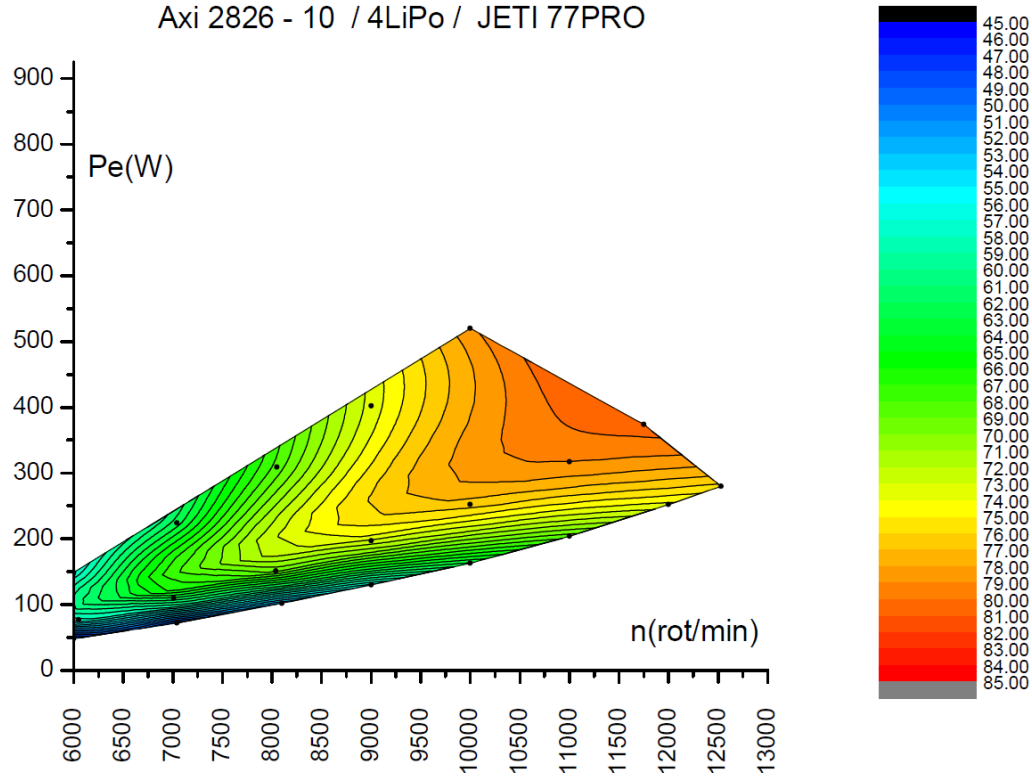

Fig. 12 AXI 2826-10 characteristics

Having the motor-propeller configuration established, from the flight telemetry data we could extract not only RPM but also the electric power. With the required propulsion power estimated above and with the motor measurements we can estimate the propeller efficiency.

8. CONCLUSIONS

We can easily determine the plane polar from the gliding flight. The more pairs (V, γ) we have meaning more flight courses that are chosen according to the selection criteria, the more precise is the drag polar. Another criteria for increasing the precision is to select gliding flight courses both at maximum and minimum speed. For a 25.694 m/s speed, a 1 m/s speed variation means a 2.2% variation of the C_X and C_Z coeficients and for a height variation of 1m (gliding path of 0.32 deg) we have a 8.7% variation of C_X and C_Z coeficients.

The Motor parameters AXI 2826/10 measured in the lab have a precision of 2% given by weight scale and electric power measurement device.

If for the horizontal flight we have the same speeds like the gliding flight and we measure both the RPM and electric power we can easily determine the required propulsion power and if we divide it to the shaft mechanical power we obtain the propeller eficiency.

These flight measurements are more likely to be used in order to determine flight trajectories than to validate theoretical results since the measurement precision is quite low.

REFERENCES

[1] C. Gong and W. N. Chan, *Using flight manual data to derive aero-propulsive models for predicting aircraft trajectories*, AIAA Aircraft Technology, Integration and Operations (ATIO) Conference, Los Angeles, CA, 1-3 Oct. 2002.

[2] D. T. Ward and T. W. Strganac, I*ntroduction to Flight Test Engineering*, Kendall-Hunt, Iowa, 2nd Edition, 2002.

[3] P. Parvu, *Mecanica aeronavei-note de curs.*

[4] * * * Learjet 60 Pilot's Manual, Learjet, Inc., Wichita, KS, July 1993, pp. 8.13-8.26.

[5] D. Raymer, *Aircraft design: A Conceptual Approach*, American Institute of Aeronautics and Austronautics, Inc., Washington, D.C., 1989,pp. 261, 269.